

This paper is a part of *Climate and environmental changes recorded in loess covers* (eds. Maria Łanczont, Przemysław Mroczek and Wojciech Granoszewski)

The anisotropy of magnetic susceptibility as a method to study Quaternary deposits: theory and applications

Artur TEODORSKI^{1, *}

¹ University of Warsaw, Doctoral School of Exact and Natural Sciences, Faculty of Geology, Żwirki i Wigury 93, 02-089 Warszawa, Poland; ORCID: 0000-0002-7893-890X



Teodorski, A., 2023. The anisotropy of magnetic susceptibility as a method to study Quaternary deposits: theory and applications. *Geological Quarterly*, 2023, 67: 50; <http://dx.doi.org/10.7306/gq.1720>

The anisotropy of magnetic susceptibility is used as a geophysical method, based on the non-uniform magnetic properties of rocks, within which it exploits the individual types of minerals, their quantity, and distribution in the rocks. The anisotropy of minerals may be a result of their crystalline structure or the shape of mineral grains. If the anisotropy is connected to the shape of the minerals, as in the case of magnetite, the axis of maximum magnetic susceptibility is perpendicular to the grain long axis. This indirectly allows determination of grain orientation in the rocks studied. Therefore, this method can be used to reconstruct the directions of transport of rock components, such as in loess, fluvial or ice-dammed sediments, and to determine the directions of ice-sheet movement based on glacial till studies. The method is also used in tectonic stress reconstruction, complementing the results of palaeomagnetic dating or the logging of borehole cores. The rapid, inexpensive measurement of anisotropy of magnetic susceptibility along with low human error in measurement has made this method competitive with traditional research methods.

Key words: Quaternary, anisotropy of magnetic susceptibility (AMS), magnetic fabric, loess, glacial tills.

INTRODUCTION

The anisotropy of magnetic susceptibility (AMS) method is a geophysical one that relies on the use of the non-uniform magnetic properties of the rocks and minerals being analysed. It has been known for over 80 years and has found many applications in geological research, including the study of Quaternary deposits. The AMS method has been used for such purposes as to reconstruct the directions of transport of rock material in aquatic environments (e.g., ice-dammed sediments) or aeolian environments (e.g., loess), the directions of ice-sheet movement using glacial tills, to reconstruct the directions of tectonic stress acting on rocks, and to complement data obtained from palaeomagnetic dating or to indicate environmental thresholds. Despite certain methodological limitations, this method has become competitive with the traditional methods used in these areas in many cases. The attributes of this method include low cost, the ease and speed of measurement, as well as a reduction in human error through automation of the measurements.

This paper reviews the theoretical assumptions of the AMS method and selected applications of this method in the study of

Quaternary deposits, reflecting its ever greater use among Quaternary researchers.

THEORETICAL ASSUMPTIONS OF THE METHOD

MAGNETIC SUSCEPTIBILITY

All substances occurring in nature react to an external magnetic field, producing a magnetization J in them, which can be described by the formula:

$$J = \chi H$$

where: χ – magnetic susceptibility; H – the value of the external magnetic field acting on a given substance (Butler, 1992).

Substances, including rocks, react differently to an applied external magnetic field and therefore have different magnetic susceptibilities, which can be described by transforming the above formula:

$$\frac{J}{H}$$

* E-mail: a.teodorski@student.uw.edu.pl

Received: May 2, 2023; accepted: October 30, 2023; first published online: February 5, 2024

Based on this formula, we can conclude that magnetic susceptibility is the proportionality coefficient between J and H and determines the ability of the substance analysed to magnetize in a given external magnetic field.

Due to their "reaction" to an external magnetic field, substances can be divided into three main groups: diamagnetic, paramagnetic and ferromagnetic (Collinson, 1983; Butler, 1992; Dunlop and Özdemir, 1997; Evans and Heller, 2003; Tauxe, 2005; Liu et al., 2012). As a result of the action of an external magnetic field, diamagnetic substances acquire weak magnetization opposite to the given field. This magnetization disappears with the removal of the magnetic field from the sample. The magnetic susceptibility for these substances takes low negative values. Examples of typical minerals classified as diamagnetic are quartz and calcite. An external magnetic field in paramagnetic substances generates magnetization consistent with the direction of the applied field and disappears with the cessation of this field. The magnetic susceptibility of paramagnetic minerals is low but greater than zero. Examples of paramagnetic minerals are pyroxenes, hornblende, olivine, biotite and muscovite. As a result of the action of an external magnetic field in ferromagnetic substances, strong magnetization is created in the direction consistent with the given field. After removing the magnetic field, their magnetization does not drop to zero, which we call remanent magnetization. The magnetic susceptibility of ferromagnetic substances is positive and much higher than that of the two previous types of substances. Examples of ferromagnetic minerals are magnetite, hematite, pyrrhotite, maghemite, goethite and greigite.

The magnetic susceptibility of rocks depends on the sum of the susceptibility of all minerals in the rock, and in particular on the type, quantity and size of ferromagnetic minerals. The susceptibility of rocks with values above 5×10^{-3} SI is controlled only by magnetite, while the susceptibility with values below 5×10^{-4} SI is controlled by paramagnetic minerals (Hrouda, 2007). The dominant influence of a particular type of mineral on magnetic susceptibility does not necessarily affect the source of magnetic susceptibility anisotropy.

ANISOTROPY OF MAGNETIC SUSCEPTIBILITY

Most substances occurring in nature have an inhomogeneous shape or internal structure. This also applies to minerals and the rocks that they build, and also affects the magnetic properties of these substances.

The ability to magnetize a magnetically anisotropic substance depends on the plane in which an external magnetic field acts:

$$\begin{aligned} M_1 &= k_{11}H_1 + k_{12}H_2 + k_{13}H_3 \\ M_2 &= k_{21}H_1 + k_{22}H_2 + k_{23}H_3 \\ M_3 &= k_{31}H_1 + k_{32}H_2 + k_{33}H_3 \end{aligned}$$

where: M_i ($i = 1, 2, 3$) - components of the magnetization vector (in the Cartesian coordinate system); H_j ($j = 1, 2, 3$) - components of the applied external magnetic field; k_{ij} ($k_{ij} = k_{ji}$) - constants representing the components of the second-rank tensor called the susceptibility tensor (Hrouda, 1982).

In the Cartesian coordinate system, the non-diagonal components of the susceptibility tensor are zero. Therefore, we can write the above equations in the form:

$$\begin{aligned} M_1 &= k_{11}H_1 \\ M_2 &= k_{22}H_2 \\ M_3 &= k_{33}H_3 \end{aligned}$$

where: k_{11} , k_{22} , k_{33} - the principal susceptibilities respectively termed the maximum (k_{max}), intermediate (k_{int}) and minimum susceptibility (k_{min}).

The tensor of magnetic susceptibility anisotropy can be graphically represented by an ellipsoid based on three mutually perpendicular principal axes corresponding to the values of k_{max} , k_{int} and k_{min} (Fig. 1). Based on magnetic susceptibility measurements in different planes, it is possible to calculate the length, direction, declination and inclination that determine the position of the principal magnetic susceptibility axes in three-dimensional space (Jelínek, 1977). In addition to the principal susceptibility axes, a series of parameters describing susceptibility and susceptibility anisotropy are determined, such as mean magnetic susceptibility $K_m = (k_{max} + k_{int} + k_{min})/3$, magnetic lineation $L = k_{max}/k_{int}$, magnetic foliation $F = k_{int}/k_{min}$, corrected degree of anisotropy [$P_j = (k_{max}/k_{min})^a$ where: $a = \sqrt{(1 - T^2 / 3)}$] and shape parameter [$T = (2\eta_2 - \eta_1 - \eta_3)/(\eta_1 - \eta_3)$, where $\eta_1 = \ln k_{max}$, $\eta_2 = \ln k_{int}$, $\eta_3 = \ln k_{min}$] (Jelínek, 1981; Hrouda, 1982).

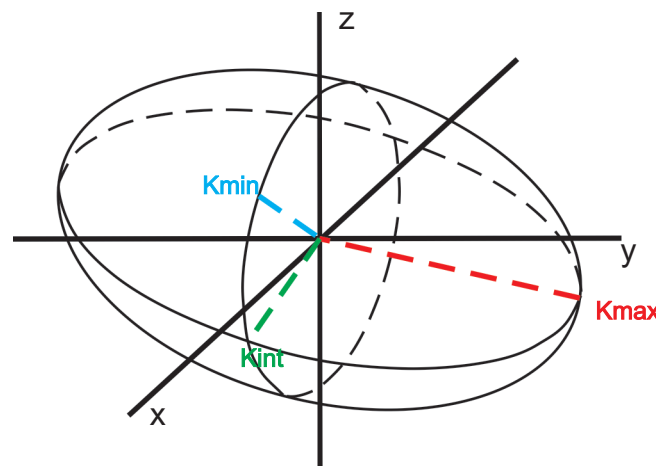


Fig. 1. Magnetic susceptibility ellipsoid with orientation of the principal magnetic susceptibility axes (k_{max} , k_{int} , k_{min})

AMS VERSUS MINERALS

Anisotropy of magnetic susceptibility (AMS) depends on the type of minerals that make up the rocks and their distribution in the rock. The magnetic anisotropy of minerals can result from the shape of the minerals or their crystallographic structure

(Hrouda, 1982; Butler, 1992; Rochette et al., 1992; Tauxe, 2005; Borradaile and Jackson, 2010; Biedermann, 2018).

The AMS resulting from the crystalline structure of minerals is called magnetocrystalline anisotropy (Butler, 1992; Tauxe, 2005). The AMS axis orientations are related to the crystal structure and symmetry, the iron content in individual minerals, and the degree of oxidation. In this type of anisotropy, magnetization M is more easily obtained in certain specific crystallographic directions (a , b , or c) due to low magnetocrystalline energy values. Therefore, magnetic susceptibility k in different crystallographic directions is different. Magnetocrystalline anisotropy is characteristic of diamagnetic (quartz, carbonates), paramagnetic (silicates), and some ferromagnetic minerals (hematite, pyrrhotite) (Borradaile and Jackson, 2010; Biedermann, 2018).

For pure diamagnetic minerals such as trigonal quartz or calcite, a specific “inverse” magnetic fabric occurs. The situation is often observed where the “longest” susceptibility axis is parallel to the elongation of the crystal. Because diamagnetic minerals have negative susceptibility, the “longest” axis is the

axis of least susceptibility, i.e., k_{min} . This means that the k_{min} axis is parallel to the elongation of crystals (crystallographic axis c) (Borradaile and Jackson, 2010; Fig. 2A). This can cause some problems in interpreting magnetic fabric. However, the AMS of rocks resulting from the presence of diamagnetic minerals is rare. A specific “inverse” magnetic fabric occurs for carbonate minerals with low iron content (<1000 ppm). Diamagnetic carbonate minerals with high iron content have k_{max} parallel to the crystallographic axis c (Biedermann, 2018).

For paramagnetic minerals with high symmetry (e.g., cubic, tetragonal, orthorhombic), the AMS axes coincide with the crystallographic axes a , b , c of the minerals (Borradaile and Jackson, 2010; Biedermann, 2018). Nesosilicates (e.g., orthorhombic olivine) are an example of such minerals (Fig. 2B). Many researchers state that the k_{max} axis is parallel to the c axis, the k_{int} and k_{min} axes are parallel to the other crystallographic axes, and their position relative to the crystal axes depends on the iron content. The AMS ellipsoid of olivine changes from prolate to more oblate with increasing iron content. Due to their high symmetry, orthopyroxenes are also characterized by AMS axes

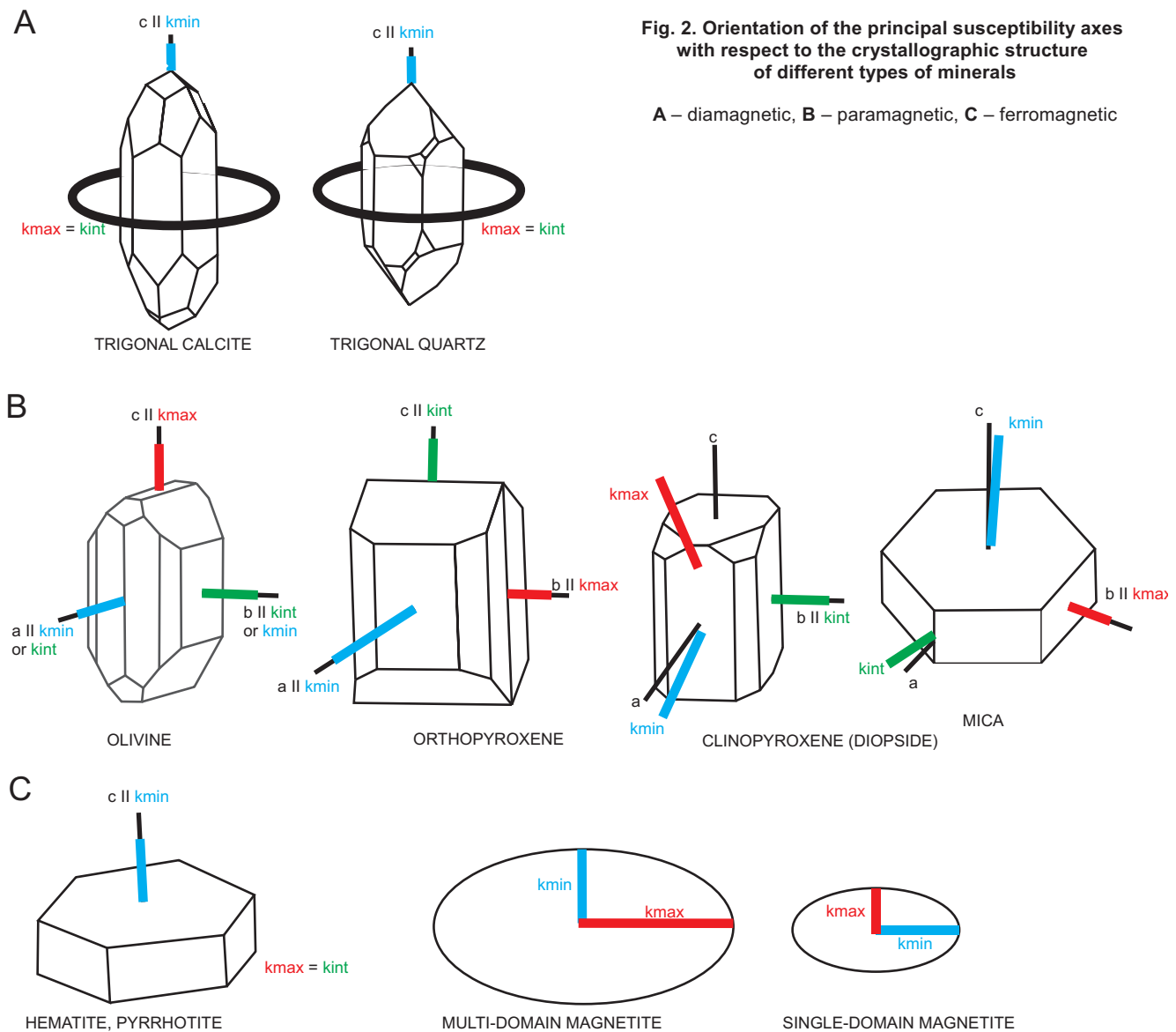


Fig. 2. Orientation of the principal susceptibility axes with respect to the crystallographic structure of different types of minerals

A – diamagnetic, **B** – paramagnetic, **C** – ferromagnetic

parallel to the crystallographic axes (Fig. 2B); however, various authors state different relationship between individual susceptibility and crystallographic axis. The AMS ellipsoid is rather prolate.

However, most paramagnetic minerals that make up rocks are monoclinic or triclinic. In such cases, the crystallographic axis orientations differ somewhat from the AMS axis orientations (Borradaile and Jackson, 2010; Biedermann, 2018). Most clinopyroxenes (inosilicates) have k_{int} parallel to the b axis, and the other axes are located in the plane formed by the a and c axes. For example, in diopside, the k_{max} axis is set at an angle of 45° to the c axis (Fig. 2B). The AMS ellipsoid of clinopyroxenes takes a varied shape. However, for micas, chlorites, and clay minerals, the k_{min} axis is almost perpendicular to the basal plane c , and in the basal plane, anisotropy is practically imperceptible; if it occurs, the AMS axes may not perfectly coincide with crystallographic axes (Fig. 2B). They have an oblate magnetic fabric.

Due to differences in AMS axis orientations and crystallographic axis orientations, even perfectly oriented paramagnetic minerals can create imperfectly oriented AMS. This can also lead to a situation where a desired AMS resulting from the arrangement of mineral grains (see magnetite) is obscured by magnetocrystalline anisotropy of paramagnetic minerals. On the other hand, for minerals that form elongated and platy grains, as previously noted, the k_{max} axis can be parallel to the elongation of grains. This is also corroborated by AMS studies in clay rocks where magnetic lineations have been observed. Clay minerals that break along the basal plane can align parallel to the stretching direction in rocks (Parés and van der Pluijm, 2002; Ciffeli et al., 2005, 2009).

Hematite, hemo-ilmenite, and pyrrhotite, which are ferromagnetic minerals, have magnetocrystalline anisotropy with k_{min} perpendicular to the basal plane (Borradaile and Jackson, 2010; Biedermann, 2018; Fig. 2C). In some cases, pyrrhotite has anisotropy resulting from its shape.

In AMS resulting from the shape of mineral grains, the susceptibility is highest in the direction of elongation of the mineral grain because magnetization is most easily obtained in this direction due to the lowest value of magnetostatic energy (Butler, 1992; Tauxe, 2005). If the anisotropy results from the shape of mineral grains, as is the case with magnetite, then the maximum magnetic susceptibility axis is parallel to the longest axis of the mineral grain (Fig. 2C). In this case, the AMS indirectly shows the arrangement of magnetic mineral grains in the rock, which can be used to reconstruct directions of transport of rock material in different geological environments, directions of magma flow or directions of tectonic stress. Large multi-domain (MD) magnetite grains are characterized by k_{max} parallel to the longest axis of the grain, while fine single-domain (SD) magnetite grains have an inverse magnetic fabric, where the k_{min} axis is parallel to the longest axis of the mineral grain (Hrouda and Ježek, 2016; Černý et al., 2020).

Dia-, para-, and ferromagnetic minerals often contain inclusions and impurities of other minerals or mineral phases that can significantly affect the magnetic properties of individual minerals.

In geological research, there are cases where the AMS obtained may come from different groups of minerals. For example, in clay rocks, the anisotropy resulting from the arrangement of paramagnetic minerals may obscure the anisotropy of ferromagnetic minerals (magnetite), which can complicate proper geological interpretation. Difficulties in interpretation can also arise from the presence of SD magnetite in samples, which may be responsible for inverse magnetic fabric. To distinguish AMS resulting from the arrangement of paramagnetic minerals from those resulting from the arrangement of ferromagnetic minerals

or to identify inverse magnetic fabric, we can use methods based on the anisotropy of magnetic residues – anhysteretic (AARM) and isothermal (AIRM) remanent magnetization (Borradaile and Henry, 1997; Borradaile and Jackson, 2010; Almqvist et al., 2012; Schöbel et al., 2013).

MAGNETIC FABRIC VERSUS ROCK FABRIC

Based on the parameter T describing the shape of the anisotropy ellipsoid, we can distinguish four types of magnetic fabric occurring in rocks (Fig. 3). The first of these occurs when $T > 0$ and is close to 1. This indicates that magnetic foliation F is significantly more prevalent than the magnetic lineation L in the resulting fabric (Butler, 1992; Tauxe, 2005). This type of anisotropy is called *oblate magnetic fabric* and is associated with the occurrence of preferentially oriented platy minerals such as clay minerals or minerals from the mica group, which also create a macroscopic foliation in rocks. Elongated magnetite grains, for example, arranged in the plane of foliation can also create foliated AMS. An anisotropy in which foliation is clearly dominant is characterized by a scattered orientation of the k_{max} and k_{int} axes in the plane of foliation and well-oriented k_{min} axes perpendicular to the plane of foliation ($k_{max} > k_{int} > k_{min}$). The second type of the anisotropy occurs when $T < 0$ and is close to -1 . In this case, L clearly dominates over F , and this anisotropy is called *prolate magnetic fabric*. This anisotropy is associated with the preferred orientation of elongated minerals, which also create a macroscopically visible lineation. This type of anisotropy is expressed by well-oriented k_{max} axes and scattered orientation of the remaining axes in the plane perpendicular to the maximum axis ($k_{max} > k_{int} > k_{min}$). *Triaxial magnetic fabric* occurs when the values of the T parameter are positive or negative, but close to 0. The principal axes of magnetic susceptibility are well-oriented on the stereographic projection in three groups ($k_{max} > k_{int} > k_{min}$). In rocks where there is no magnetic anisotropy, *isotropic magnetic fabric* occurs. In this case, the anisotropy ellipsoid is a sphere, and the susceptibility axes are randomly distributed on the projection ($k_{max} \approx k_{int} \approx k_{min}$). This means that the minerals constituting the rocks do not exhibit any preferred orientation.

To determine whether the orientation of AMS axes is consistent with the rock fabric, the orientation of the principal susceptibility axes is compared with rock fabric elements visible macroscopically, such as measurements of the orientation of long pebble axes, orientation of sand grains in thin sections, sedimentary structures or orientation of tectonic structures, etc. (see below). The results of AMS are also compared with more advanced research methods that allow determining the preferred crystallographic orientation of minerals, such as X-ray pole figure goniometry or neutron texture goniometry. A correlation has been observed between the orientation of phyllosilicate and AMS fabric resulting from the arrangement of paramagnetic minerals (Lüneburg et al., 1999; Parés and van der Pluijm, 2003; Chadima et al., 2004; Ciffeli et al., 2009; Kuehn et al., 2019). Similarities between the mineral fabric and magnetic fabric have also been observed in amphibole-bearing rocks (Biedermann et al., 2018) and carbonate rocks (Schmidt et al., 2009). This shows that AMS can be used to determine rock fabric.

TYPE OF AMS SAMPLES AND SAMPLING METHOD

Samples for AMS analysis should be taken from unweathered sediments and rocks. Three types of sample are used in AMS studies. The first are cylindrical samples with a standard diameter of 2.54 cm and a height of 2 cm. This kind of sample is

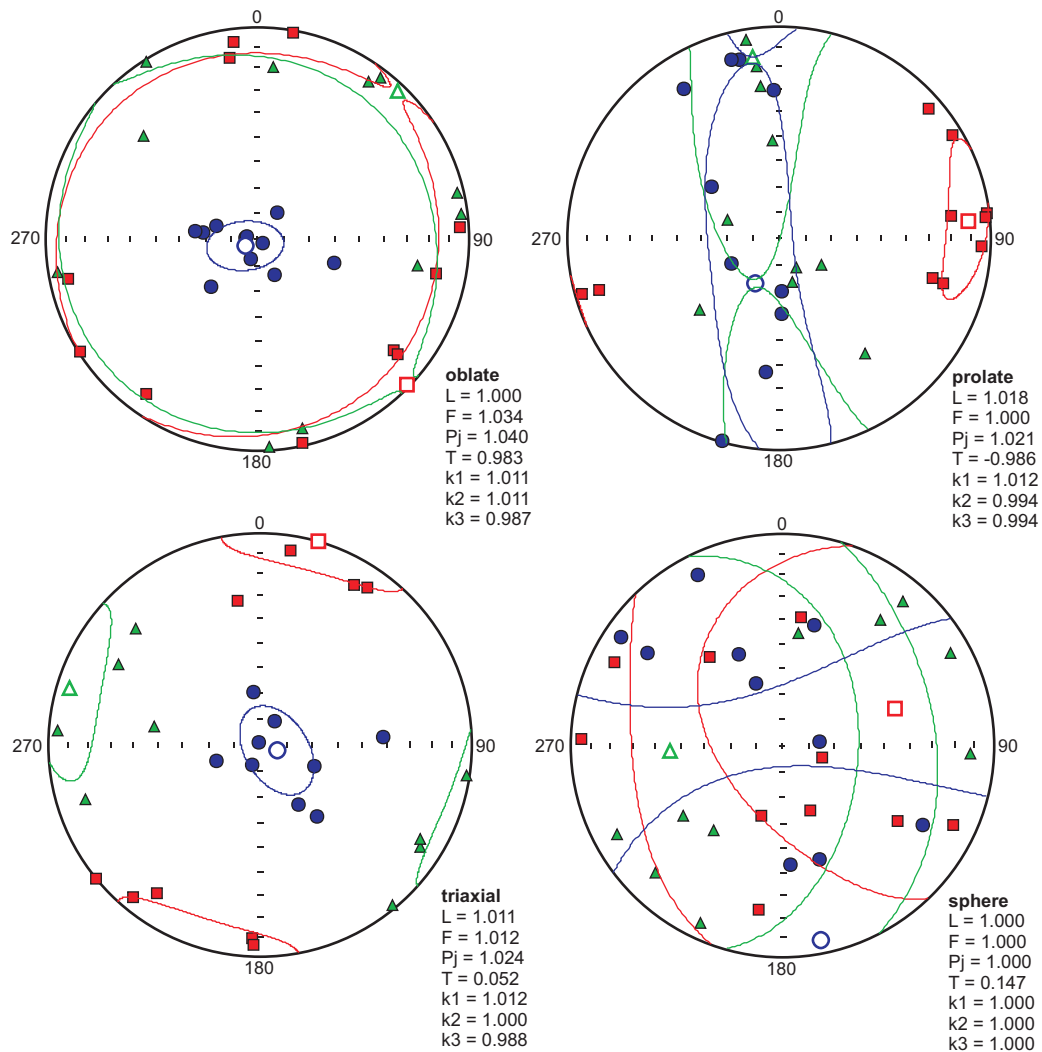


Fig. 3. Types of magnetic fabric

Red squares – k_{max} , green triangles – k_{int} , blue circles – k_{min} ; L – magnetic lineation, F – magnetic foliation, P_j – corrected degree of anisotropy; T – shape parameter; k_1, k_2, k_3 – semi-axes of mean susceptibility tensor

obtained from lithified rocks such as limestone or basalt or unlithified sediments such as loess, tills, or clays. Cubic samples with dimensions of 2 x 2 x 2 cm are also used, which are most often cut from rock blocks. Plastic boxes with a shape similar to a cube are also prepared to collect samples from borehole cores (e.g., in lake sediments) (Rosenbaum et al., 2000; Liu et al., 2001; Yang et al., 2019) or soft sediments collected from exposures (Gentoso et al., 2012; Ankerstjerne et al., 2015; Ives, 2016).

The AMS samples in the forms mentioned above can be taken directly from a previously cleaned exposed wall. A variety of tube samplers (Nawrocki, 2006; Teodorski et al., 2021) made of brass, for example, are used to collect sediment cores. The cores obtained can be hardened with sodium silicate before being cut to the standard AMS sample size. Cores may be sampled from solid rocks using mechanical coring drills (Cifelli et al., 2004; Fleming et al., 2013a; Caricchi et al., 2016). Samples of poorly lithified rocks and deposits can also be taken in the form of blocks, which are optionally stabilized with sodium silicate (Maffione et al., 2012; Fleming et al., 2013b; Brádko et al., 2018b). Hardening may be achieved by stabilizing the desired sediments or rocks in the exposed wall (Anastasio et al., 2021).

This applies mainly to deposits characterized by significant porosity because penetration and solidification of sodium silicate take less time. For clays, Kubiena cans can be used (Thomason and Iverson, 2009; Hopkins et al., 2016), and then the blocks obtained can be saturated with sodium silicate in the laboratory. Next, standard-sized AMS samples are cut from the resulting block. For lithified rocks, manual blocks can be taken, from which individual AMS samples are cut in a laboratory. The AMS samples must be oriented relative to the three-dimensional coordinate system and north using a compass. Additionally, the strike and dip of the rock layers from which the samples were taken can be measured for tectonic correction.

SELECTED HISTORICAL USES OF THE AMS METHOD IN SEDIMENTARY RESEARCH

The first description of magnetic susceptibility anisotropy comes from the work of Swedish researcher Gustaf Ising (1942), who studied Swedish varved clays. He found that the

magnetic susceptibility measured parallel to the lamination of the clays is greater than that measured perpendicular to the lamination, which is evidence of the anisotropic structure of rocks and the minerals that are activated in the applied field.

After World War II, numerous laboratory studies were conducted to understand the depositional mechanisms responsible for a given type of AMS. King (1955) conducted laboratory work that involved determining factors affecting the orientation of magnetic mineral grains other than those associated with the Earth's magnetic field. The studies were carried out using a water tank in which suspensions of silt from Swedish varved clays were deposited in a magnetic field generated by magnetic coils. King (1955) found that in addition to the Earth's magnetic field, other factors affecting the arrangement of mineral grains, and thus the interpreted directions of magnetization, are the angle of inclination of the surface on which sediments are deposited and the possible presence of water currents.

In connection with the conclusions drawn from King's (1955) experiments, researchers began to search for a method that could help identify mechanical factors affecting the arrangement of mineral grains. Numerous laboratory studies were conducted by Rees (1961). He examined the influence of water currents acting during sediment deposition on the record of magnetization directions in the sedimentary layers. Once again, silts from Swedish varved clays were analysed. He found that in many cases the magnetization vector lies in the same direction as the maximum susceptibility axis because magnetic grains are most easily magnetized in the direction of their greatest elongation (Rees, 1961). He suggested that based on the arrangement of the maximum magnetic susceptibility axis, it is possible to correct the magnetization directions obtained in sediments deposited from water currents. The results of his laboratory experiments were transferred to studies of sediments deposited in nature. He conducted research on varved clay samples from the Stockholm area. By examining the natural remanent magnetization (NRM) of the clays, he found that the magnetization vector obtained for the same age varves, indicated by local varvochronology, was different at two different sites. Because the varves studied were synchronous this phenomenon could not be explained by an excursion of the Earth's magnetic field pole. According to Rees (1961), water currents with different directions that affected the arrangement of deposited mineral grains had an impact on the different magnetization directions obtained. This was demonstrated by noting the diverse orientations of the k_{max} in contemporaneous varves and the orientations of landforms indicating the direction of water inflow into the basin (Rees, 1964). Rees (1965) conducted further research on contemporary beach sediments from Scripps Beach and Pliocene heterogeneous deposits (from clay to gravel) from Santa Paula Creek in California. In beach sands, he found that the orientation of k_{max} is identical to that of longer mineral grain axis. In the Pliocene deposits, he noted that the k_{max} orientation indicates a similar direction of water currents as determined from orientations of cross-bedding, shell fragments and sole markings. His research showed that the AMS method can be an alternative to traditional macroscopic and microscopic methods for determining directions of rock material transport (Rees, 1965). Rees (1966) also conducted laboratory research on the influence of deposition on the arrangement of mineral grains and AMS. Again, he conducted research on sands from Scripps Beach. The research showed that magnetic foliation planes are inclined in the same direction as the bed on which the sediments were deposited, but with a smaller inclination.

With increasing substrate inclination (α), the degree of k_{max} orientation (magnetic lineation consistent with substrate inclination direction) and the degree of grain orientation observed in thin sections increase; that is, in addition to foliation, we have an increasing share of lineation. Rees (1966) noted that sediments deposited on a steep slope characterized by a more pronounced magnetic lineation may be confused with sediments deposited through the involvement of water currents. The linear arrangement of grains may be related to sediment movement down the slope (Rees, 1966).

In the early 1960s, the first work on the use of AMS in glacial till studies was also carried out (Fuller, 1962) on tills from Barrington chalk pit (Cambridge, England). He was the first to state that AMS can be used to determine the arrangement of magnetic minerals in glacial tills. He showed that the axis of maximum magnetic susceptibility is parallel to the arrangement of the longer axis of pebbles as well as sand grains. Based on these observations, he concluded that the AMS method can be used to determine the directions of ice-sheet movement.

The AMS method in loess has a briefer application compared to other geological materials. This is because it was more difficult to develop a proper method for sampling poorly consolidated deposits such as loess. The first publications on this subject began to appear in the 1980s. One of them was by Liu et al. (1988), describing research at a site near the Chinese town of Xifeng. Originally deposited loess, redeposited alluvial sediments from loess, and red clays underlying loess were studied. The authors characterized magnetic fabrics in the loess studied for which anisotropy resulting from foliation is typical. The axis of minimum susceptibility is perpendicular to the surface on which the loess was deposited, with a deviation from the vertical of $<15^\circ$. They also found that a primary magnetic fabric characteristic for the loess studied also occurs in palaeosols. However, the values of magnetic anisotropy are slightly lower for paleosols than for loess, despite the presence of hematite – which is characterized by strong magnetocrystalline anisotropy – in palaeosols. Based on magnetic fabrics and other magnetic properties, it was possible to distinguish loess from alluvial deposits and also to determine that the red clays underlying loess have an aeolian genesis, which was corroborated by additional macroscopic studies.

EXAMPLES OF APPLICATION OF AMS METHOD IN STUDIES OF QUATERNARY DEPOSITS

LOESS

Based on the type of magnetic fabric in loess, several depositional or post-depositional processes can be determined (Bradák-Hayashi et al., 2016; Bradák et al., 2020):

- Magnetic fabrics characterized by scattered k_{max} and k_{int} along the horizontal plane and well-oriented vertical k_{min} which are deposited mainly through gravitational forces (Tarling and Hroudá, 1993; Hus, 2003; Baas et al., 2007; Wang and Lrvlie, 2010);
- Magnetic fabrics with well-oriented principal axes of magnetic susceptibility in aeolian deposits, where the orientation of the k_{max} and/or imbrication of k_{min} axes indicates the direction of aeolian material transport (e.g., Ge et al., 2014; Zeeden et al., 2015; Obersteinová, 2016; Xie et al., 2016;

Nawrocki et al., 2019); the imbrication of the k_{min} axis usually does not exceed 20° ; with strong winds, the k_{max} axis may be oriented perpendicular to the wind direction (Lagroix and Banerjee, 2004; Nawrocki et al., 2006);

- Magnetic fabrics indicating sediment deposition on a slope and/or material transport down a slope (Bradák-Hayashi et al., 2016; Bradák et al., 2020); the k_{min} axis is well-oriented, and the other axes are characterized by greater dispersion; the imbrication of the k_{min} axis exceeds 20° ;
- Magnetic fabrics within palaeosols that have the character of primary fabrics recorded in loess or may have the character of an “inverse magnetic fabric”, where the k_{max} axis is oriented almost vertically, which may be related to the occurrence of fine super paramagnetic single-domain magnetite produced by soil bacteria (Jordanova et al., 1996; Lam et al., 2010; Li et al., 2010; Bradák et al., 2018b; Hrouda et al., 2018);
- Magnetic fabric changed by other post-depositional processes such as permafrost activity (Lagroix and Banerjee, 2004; Taylor and Lagroix, 2015), pedogenetic processes (Liu and Sun, 2012; Taylor and Lagroix, 2015; Bradák et al., 2018a), the formation of new magnetic minerals (Hrouda et al., 2018) and bioturbation (Taylor and Lagroix, 2015).

Correct interpretation of magnetic fabric types is crucial in further stages of research. In loess, AMS can be used to reconstruct palaeowind directions during loess deposition. The palaeowind directions can be determined based on magnetic lineation, i.e. the orientation of k_{max} and/or based on the imbrication of the k_{min} axis.

An example of the reconstruction of aeolian transport directions using the imbrication of the k_{min} axis was described by Nawrocki et al. (2006), studying loess sites in Poland and western Ukraine. The loess analysed was deposited during the Weichselian Glaciation, and was found to have a typical oblate AMS ellipsoid resulting from the predominance of foliation over lineation. Magnetic fabrics indicated that the mean direction of the k_{min} axis is inclined from the vertical by $4\text{--}16^\circ$. In most of the sites studied, the minimum susceptibility axes are character-

ized by an imbrication towards the east or north-east. Based on the imbrication of the k_{min} axis in the sites studied, Nawrocki et al. (2006) concluded that the wind during loess deposition blew from the west or south-west (Fig. 4), a direction described as consistent with the orientation of the ice-sheet front of the Weichselian Glaciation and with the course of the Carpathians and Podolian Upland. This direction is also generally consistent with results obtained by Chlebowski et al. (2000) and Nowaczyk (2002). In summary, when mineral grains in loess are characterized by some inclination, it may be concluded that the wind during loess deposition blew from a direction opposite to that of imbrication of minimum magnetic susceptibility.

Reconstructions of aeolian transport directions based on magnetic lineations were carried out by Zhang et al. (2010). The research was conducted on three profiles of the youngest loess located in the western and central part of the Chinese Loess Plateau. Again, foliation predominates over lineation in the loess studied. Although the orientation of k_{max} axes in the profiles studied is characterized by a large dispersion and a small inclination, one can notice a certain peak of orientation density of these axes falling in the SE direction for Xifeng and Yichuan and SSE for Baicaoyuan. According to the authors, this indicates the transport of aeolian material by wind from the SE or SSE direction. The authors chose the k_{max} axis for reconstructing transport directions because the orientation of magnetite grains is responsible for the magnetic lineation. Magnetite anisotropy resulting from grain shape gives more reliable information about the arrangement of mineral grains in loess. Generally, wind direction from SE is associated with the summer monsoon. Strong summer monsoonal wind transported dust and re-oriented mineral grains deposited during the winter monsoon blowing from the opposite direction.

AMS studies have also been conducted on the loess island of Korzecko located near Chęciny in the Holy Cross Mountains (Fig. 5). The loess rests on the southeast slope of Grzywy Korzeczkowskie (Dzierżek et al., 2022). Based on correlation with other loess sites in the region, it corresponds in age to the youngest loess from the Weichselian Glaciation. Drilling sho-

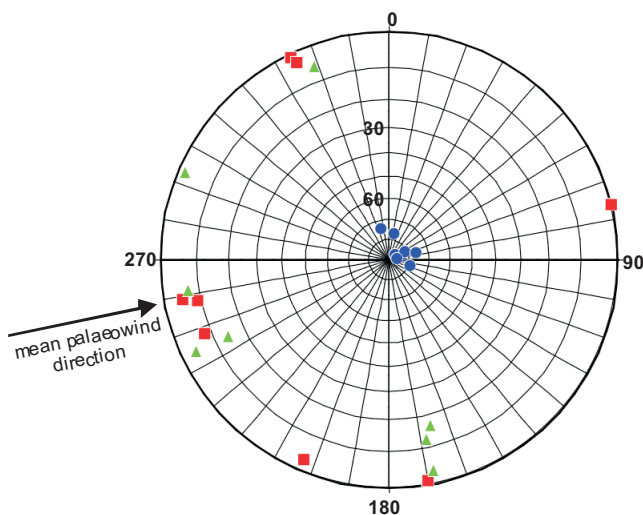


Fig. 4. Mean orientations of the principal magnetic susceptibility axes (red squares – k_{max} , green triangles – k_{int} , blue circles – k_{min}) in loess based on Nawrocki et al. (2006) along with the determined mean palaeowind direction during loess deposition (black arrow)



Fig. 5. Location of the study site on the map of Poland showing the extent of the Vistulian Glaciation (after Marks et al., 2016)

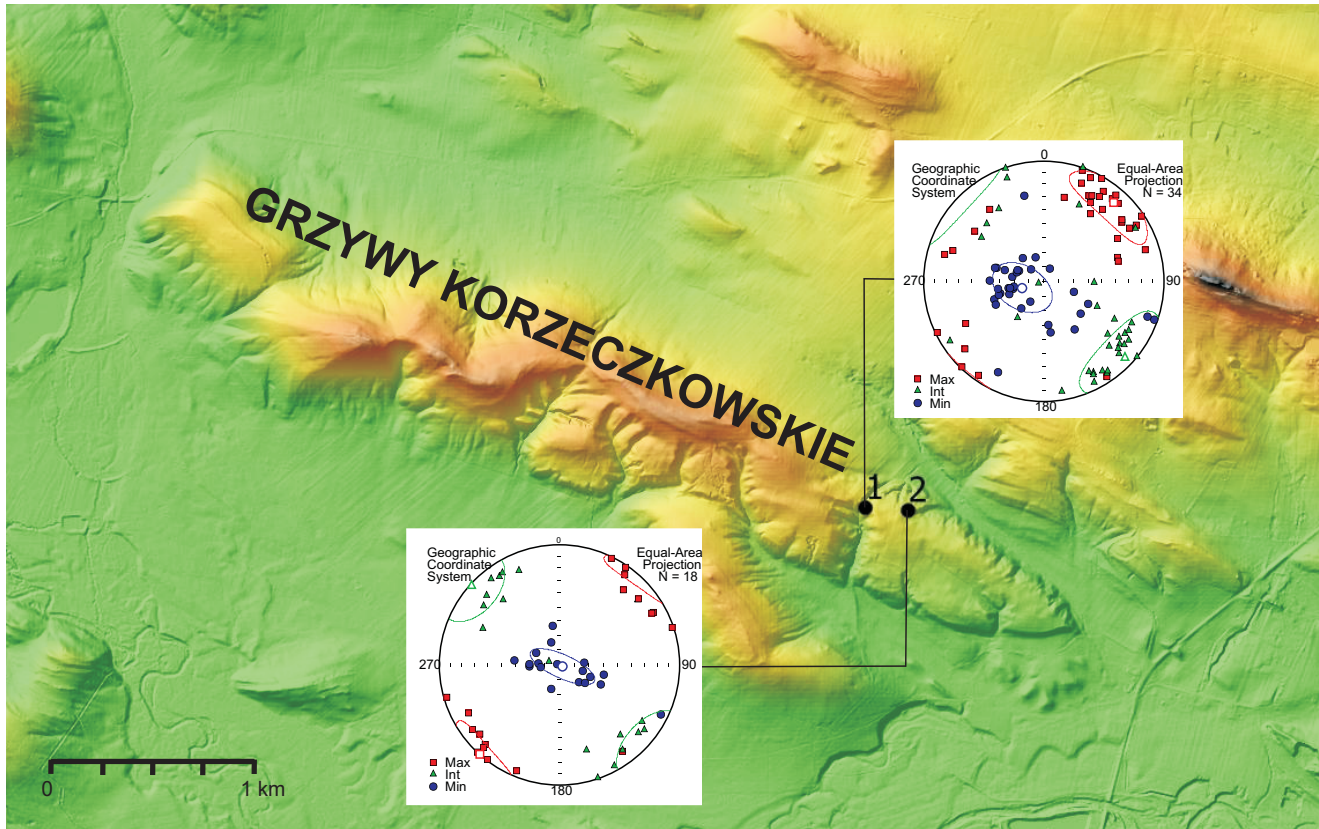


Fig. 6. Results of AMS studies in the loess of Grzywy Korzeczkowskie

1 – GK 1 site, 2 – GK 2 site

wed the thickness of loess in the vicinity of Korzecko to be 10 m. The upper 2.5 m of the loess profile at two locations (GK 1 and GK 2) were studied using AMS. The mean orientation of k_{max} is $41/13^\circ$ for GK 1 and $222/1^\circ$ for GK 2 (Fig. 6). Despite the large angle of imbrication in GK1, which may suggest deposition of loess on a slope, both locations have a similar orientation of magnetic lineation. Similarities in the orientation of the maximum susceptibility axis suggest that loess accumulation here was influenced by winds from the north-east.

GLACIAL TILLS

AMS has been used in glacial till to determine the direction of ice-sheet movement (Gentoso et al., 2012; Król and Wachacka-Kotkowska, 2015; Hopkins et al., 2016; Teodorski et al., 2021), obtain new data concerning the origin of glacial forms (Ankerstjerne et al., 2015; Hopkins et al., 2015; Ives, 2016; McCracken et al., 2016), determine the degree of subglacial deformation (Shumway and Iverson, 2009; Thomason and Iverson, 2009; Fleming et al., 2013a; Narloch et al., 2021), and describe glacetectonic structures (Fleming et al., 2013b)

An important contribution to the use of AMS in glacial till investigations was made by Hooyer et al. (2008), whose laboratory studies involved applying simple shear with increasing magnitude to glacial tills using a ring-shear device and observing changes in the magnetic fabrics of the tills. Deformation of

the ice-sheet bed resulting from simple shear is a common mechanism of ice-sheet movement (Clark, 2005). Two basal tills from the Wisconsin Glaciation (Douglas till and Batestown till) were used for the study. No direct correlation was found between increasing magnitudes of shear strain, the degree of anisotropy and the shape parameter of the anisotropy ellipsoid. However, a strong correlation was observed in the degree of ordering of the principal magnetic susceptibility axes, especially the k_{max} axis. The eigenvalue S_1 , which determine the degree of clustering of the k_{max} axes around the mean vector, increases with increasing shear forces until critical strains are reached at high shear strain magnitudes. For the Douglas till, S_1 values for critical strains are 0.75, and for the Batestown till they are 0.83. In the initial phase of the experiment, when no shear strain acts on the tills studied, magnetic susceptibility axes are characterized by a chaotic scatter (Fig. 7). As the applied shear forces increase, susceptibility axes begin to become increasingly ordered. At intermediate shear strain magnitudes, k_{max} axes undergo reorientation along the shear plane orientation. At high shear strain magnitudes, a well-defined orientation of the k_{max} axis is parallel to the direction of applied shear forces with an inclination of $18\text{--}26^\circ$ in the opposite direction to the direction of applied shear forces; the k_{int} axis lies parallel to the shear plane and perpendicular to the direction of applied shear forces; and the k_{min} axis lies in the same line as the k_{max} axis and is characterized by some imbrication consistent with the direction of applied shear forces. The experiment indicated that AMS can be used to determine the direction of applied shear forces and

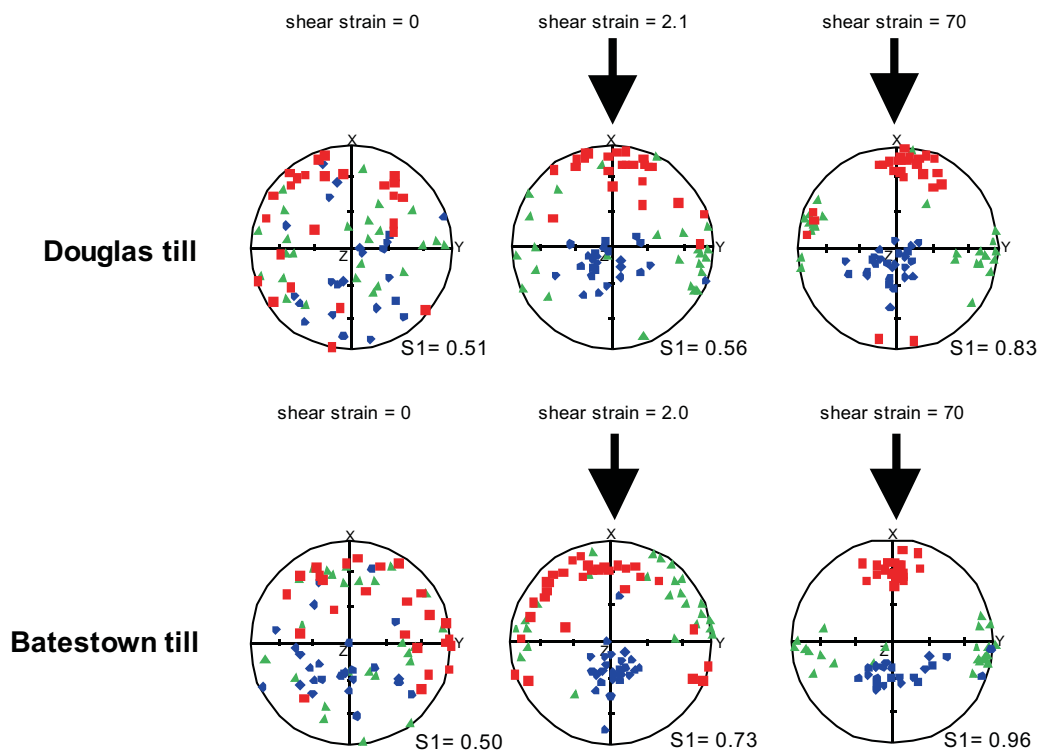


Fig. 7. Selected results of Hooyer et al. (2008) research on glacial tills
 squares – k_{max} , triangles – k_{min} , circles – k_{int} , black arrow – direction of shear forces

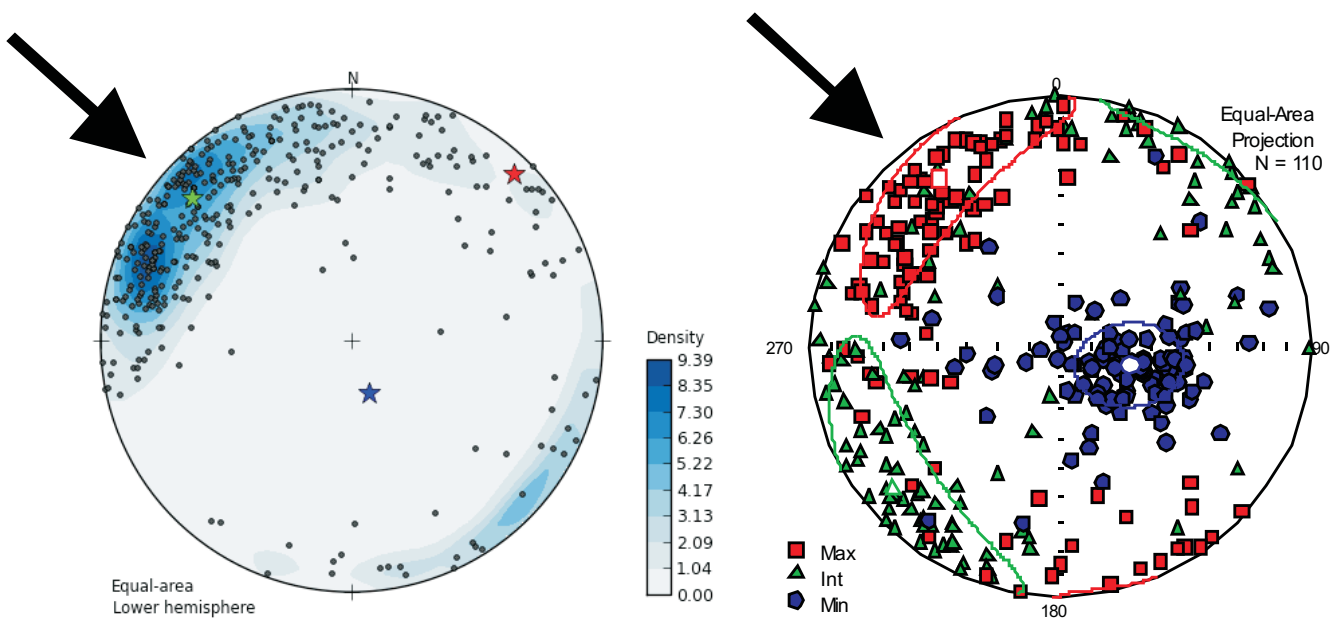


Fig. 8. Comparison of measurements of the longer axis of pebbles (left) and the orientation of the principal susceptibility axes (right) in glacial tills based on Teodorski et al. (2021)

Interpreted direction of ice-sheet movement is marked by a black arrow

hence ice-sheet movement direction. The type of magnetic fabrics in glacial tills may also indicate the magnitude of applied shear forces.

The results of laboratory tests have been applied to the study of glacial tills. An example of the use of laboratory test results is the study of glacial tills from the Douglas Member belonging to the Miller Creek Formation (Shumway and Iverson, 2009). These tills were taken from exposures above Lake Superior in northwestern Wisconsin. AMS studies aimed to determine the conditions of till deposition, and in particular to reconstruct the directions and magnitudes of shear strain during till deposition. Based on the degree of k_{max} orientation ($S_1 > 0.75$), it was found that the tills investigated mostly accumulated with subglacial deformation and shear strain causing critical deformation in them. The mean azimuth of the k_{max} axis was 17° , indicating ice movement from the NNE, consistent with the general direction of ice movement in this region. The inclination of the k_{max} axis is 17° and is similar to that obtained during laboratory tests. Based on the orientation of susceptibility axes, it was also found that shear planes are characterized by a practically horizontal orientation, as indicated by, among other things, the inclination of the k_{int} axis (the axis lying in the shear plane) which is 2° .

AMS has also been used to reconstruct the conditions of deposition of glacial tills in studies of two till layers from the Saalian Glaciation in the Dębe area in central Poland (Teodorski et al., 2021). Based on the measurements carried out, a large similarity was found in the orientation of the longer axis of pebbles ($V_1 = 312/16^\circ$) occurring in tills and the orientation of the maximum magnetic susceptibility axis ($k_1 = 324/19^\circ$) (Fig. 8). Both methods indicate that the direction of ice-sheet movement was from the NW, the regional direction of ice-sheet movement in this area. Based on magnetic fabrics, it was found that ice-sheet movement occurred through subglacial deformation expressed by shear.

STRUCTURAL ANALYSIS

The AMS method can also be used to identify tectonic deformation recorded in sediments and rocks (e.g., Mattei et al., 1997; Borradaile and Hamilton, 2004; Parés, 2015). The long axis of mineral grains in rocks tends to align along the direction of the greatest extension. Therefore, magnetic lineation can indicate the direction of the stretching acting on these rocks. In a

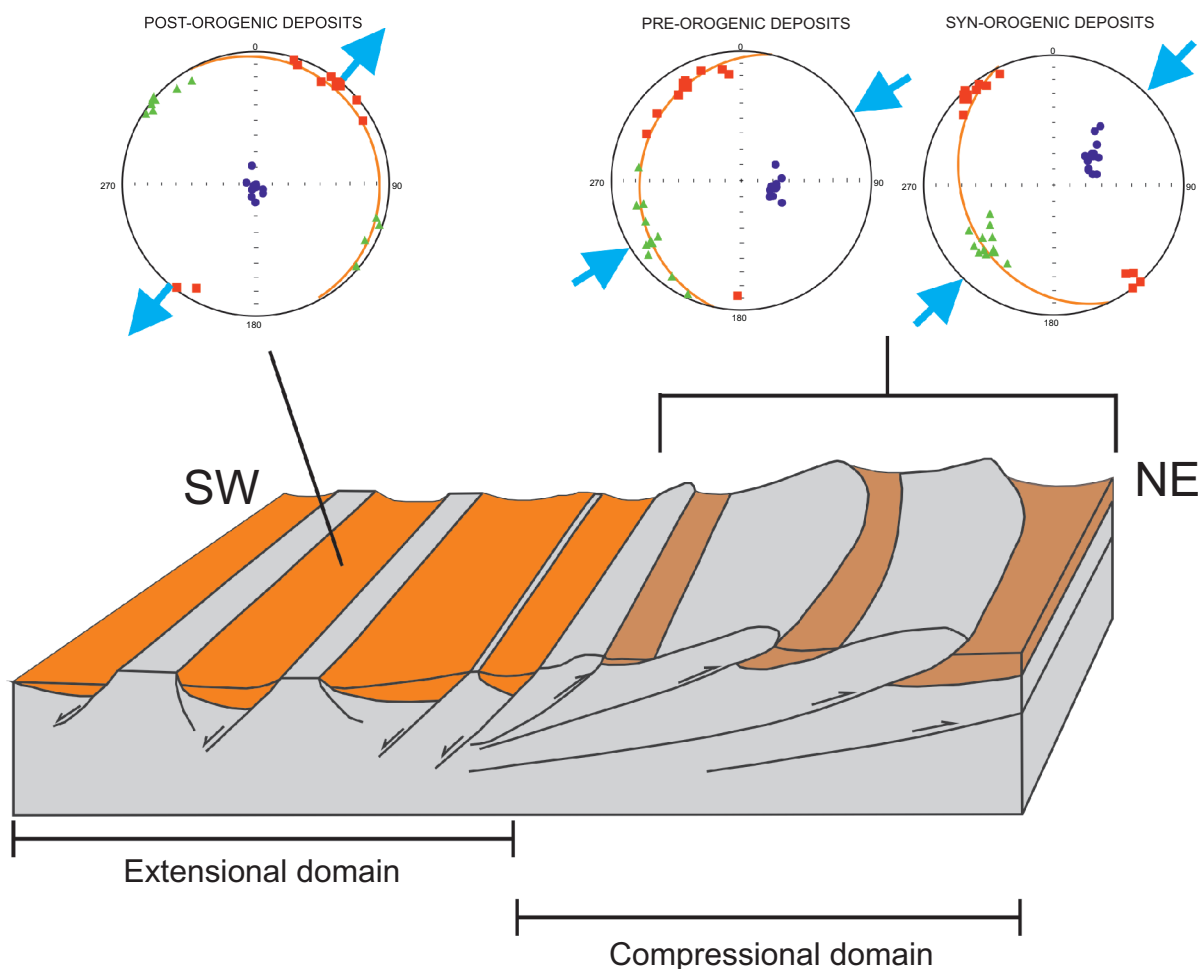


Fig. 9. Magnetic fabric and directions of tectonic deformation in compressional and extensional domains, based on Caricchi et al. (2016)

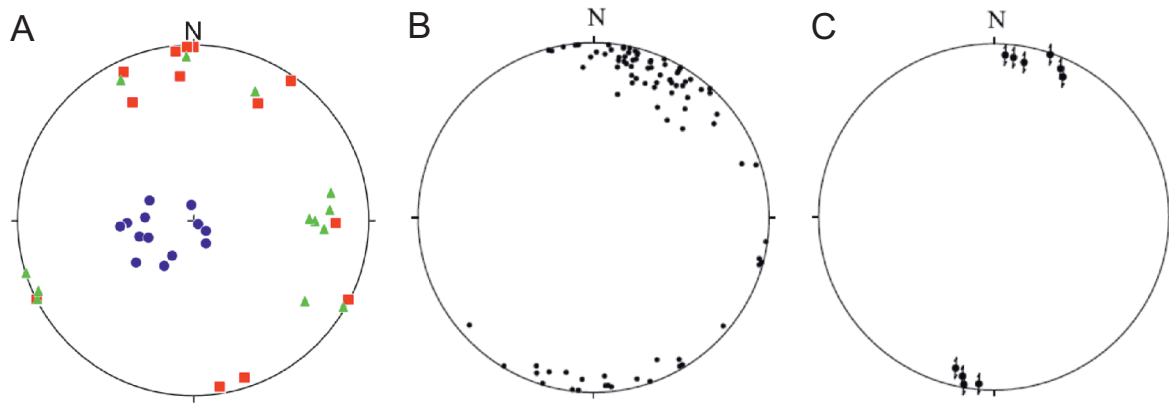


Fig. 10. AMS results (A: red squares – k_{max} ; green triangles – k_{int} ; blue circles – k_{min}), the orientation of fold axes (B), and the orientation of stretching lineations in the lower part of the Bacton diamictons based on Fleming et al. (2013b)

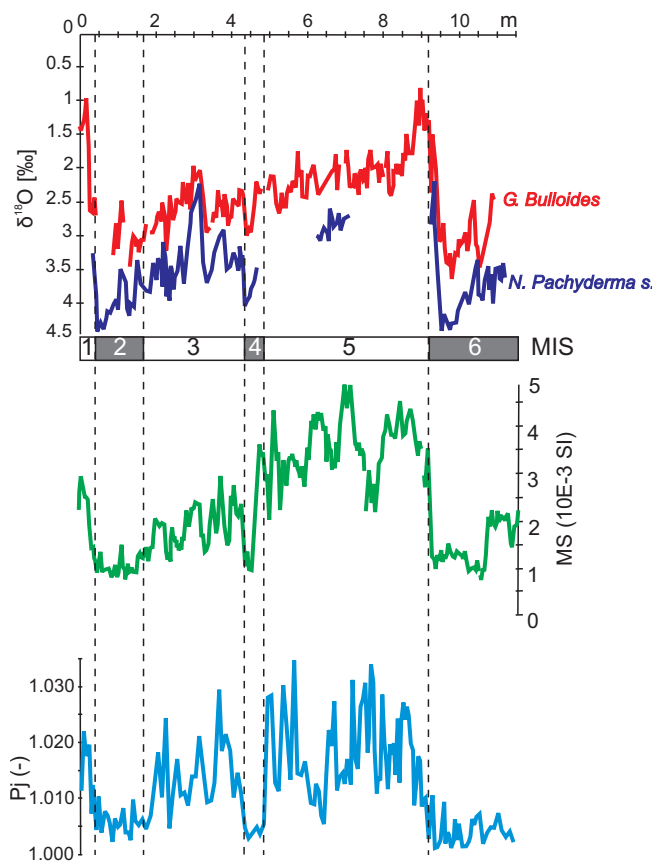


Fig. 11. Selected results of research conducted on the SU90-33 borehole core by Kissel et al. (1997); from top: $\delta^{18}\text{O}$ measurements on planktonic foraminifera, magnetic susceptibility (MS) measurements and degree of anisotropy (P_j) measurements

compressive tectonic stress regime, magnetic lineation is parallel to the orientation of fold axes, thrust faults or bedding strikes. In contrast, in an extensional regime, lineation is perpendicular to normal faults and parallel to bedding dip direction (e.g., Balsamo et al., 2008; Cifelli et al., 2009; Olivia-Urcia, 2010; Maffione et al., 2012; Tang et al., 2012; Anastasio et al., 2021).

A good example of using the AMS method in such research is a study conducted in the northern Apennines (Caricchi et al., 2016), where the method was also tested on unconsolidated deposits, as characteristic of most Quaternary successions. These studies consisted of analysing magnetic fabrics, and in particular the characteristics of magnetic lineations in areas with compressive and extensional tectonic regimes, from the northern Apennines to the Tuscan Tyrrhenian margin. The northern Apennines formed as a result of the collision of the Adria microplate with Europe. Within the Apennine chain, there are compressional zones with thrust faults. To the west of the mountain range, there is an extensional tectonic basin (the Tuscan Tyrrhenian margin) with normal faults located within it, associated with the opening of the Tyrrhenian Sea basin. AMS samples were taken from rocks forming the Apennine chain – pre-orogenic pelagic shales and marly shales, synorogenic turbidites, and from marls and sandstones from a thrust-top basin. Samples of blue clays filling the extensional postorogenic basin were also taken. In all locations studied, the rocks are characterized by magnetic fabrics with well-developed foliation parallel to the bedding planes. The foliation is related to sedimentation and subsequent compaction processes. In addition to the well-developed foliation, well-developed lineations were recorded at many sites. In the Apennine chain, magnetic lineations gradually change orientation from N–S in the south to NW–SE in the north and are parallel to the main tectonic structures of the chain. The magnetic lineations parallel to the orientation of thrust faults and fold axes indicate that the direction of compression occurring in the rocks is perpendicular to the orientation of the lineation (Fig. 9). In the postorogenic extensional basin (Tuscan Tyrrhenian margin), magnetic lineation is oriented from NE–SW to E–W, i.e. almost perpendicular to the orientation of normal faults in this area. In this case, the magnetic lineation indicates the direction of extension occurring in the rocks studied. The relationship between the orientation of magnetic lineation and the course of the main tectonic structures in rocks of different types, with different magnetic mineralogies, and also different ages, indicates that the lineation has a tectonic character.

Similar conclusions were reached by researchers into the southern Apennines (Porreca and Mattei, 2012). Samples from macroscopically undeformed clay units, mudstones and volcanic ashes, filling three small sedimentary basins in the Picentini Mountains in the southern Apennines and developed on the hanging wall of normal faults in the Plio-Pleistocene succes-

sion, were used for the study. The researchers found that in the units studied, in many cases, the primary sedimentary magnetic fabric (k_{min} perpendicular to the bedding plane, remaining axes scattered in the bedding plane) was partially overwritten by a tectonic magnetic fabric. In addition to the well-developed foliation, magnetic lineation was also observed (orientation of the k_{max} axis). A similar type of fabric was obtained in all sedimentary basins studied, regardless of lithology. This indicates that the existence of lineation does not depend on the type of rocks or on magnetic mineralogy. The magnetic lineations are well oriented along NNE–SSW or NE–SW lines. According to the authors, the magnetic lineations in the deposits studied resulted from tectonic processes, and the orientation of lineations is perpendicular to the course of normal faults interpreted in the study area. This indicates that the magnetic lineations show the direction of extension acting on the deposits studied, which led to the formation of sedimentary basins. This and the example noted above indicate that AMS studies can be used to reconstruct the directions of tectonic deformation in rocks and sediments that do not contain macroscopic tectonic structures.

Based on this method, structural analysis can also be performed in glacial deposits (Fleming et al., 2013b). The AMS method was found useful for determining the origin of glacio-tectonic structures in deformed Pleistocene deposits in northern Norfolk (near Bacton) in England. Diamictos belonging to the Bacton Green Till Member, which are part of the Sheringham Cliffs Formation, were sampled. The results of AMS studies were compared with the results obtained from classical macroscopic structural analysis performed on the exposure. In the samples studied, foliation prevails over magnetic lineation. The minimum susceptibility axis is perpendicular to the bedding and deviates from the vertical. Magnetic lineation is variable in the profile studied. It is oriented N–S ($2/6^\circ$) in the lower part and E–W ($267/6^\circ$) in the upper part. In the deposits studied, some glaciotectonic structures were indicated: sheath folds with axial planes parallel or almost parallel to the bedding, their fold axes lying almost parallel to the orientation of magnetic lineation (Fig. 10); boudinage; stretching lineations with orientation almost parallel to fold axes and magnetic lineation; sand lenses, where the deposits are characterized by orientation of the k_{max} axis parallel to the stretching lineation. According to the authors, the deposits studied underwent shear in a subglacial environment as indicated by boudins, sheath folds and stretching lineations. In the initial stage of folding, the shear was expressed by compression and the formation of initial folds. Next, the folds became more asymmetrical and characterized by axial planes almost parallel to the shear plane and tending to change fold axis orientation to parallel to the shear direction. By comparing the relationship between the k_{max} axis and the tectonic structures, it was shown that the magnetic lineation indicates the direction of extension in the shear zone. The directions of shear are identical to the directions of movement and allowed determination of the directions and timing of the advance of North Sea ice and British ice.

OTHER APPLICATIONS OF THE AMS METHOD

The AMS method has also been used in studies of changes in ocean circulation in the North Atlantic during glacial-interglacial cycles (Kissel et al., 1997). The research was carried out on a borehole core SU90-33 drilled in the North Atlantic, south of Iceland. The core consisted of muddy clay and carbonate ooze with levels of silty mud. An 11.5 m core dated to the MIS 1-6 pe-

riod was sampled. The research indicated that higher magnetic susceptibility values are characteristic of warm periods (Fig. 11). Changes in susceptibility are due to variable magnetite content, which according to the authors came from erosion of volcanic provinces such as Iceland. This was then transported and deposited in the study area by ocean currents. The authors also observed no significant variability in the size of magnetic mineral grains. The degree of anisotropy also reaches higher values in warm periods than in cold ones. According to the authors, the increase in values of the degree of anisotropy may be related to an increase in the intensity of ocean currents that influenced better orientation of mineral grains in the deposits studied. The study showed that, during cold periods, ocean circulation in this area was lower than during warm periods.

Using the AMS method, Yang et al. (2019) reconstructed types of magnetic fabrics that depend on the kind of deformation of the unconsolidated deposits in the cores. The deposits were taken from two cores drilled in the Indian Ocean area near Sumatra, and comprise mainly clays and calcareous clays, as well as silts and sands from the early Pleistocene to the present. AMS samples were taken from core segments with undeformed deposits and from drilling-deformed segments. The undeformed deposits were found to be characterized by magnetic fabrics with a well-oriented k_{min} perpendicular to bedding and the remaining axes scattered in the bedding plane, which is the result of deposition and subsequent compaction of the deposits. The magnetic fabric in deformed core sections may be influenced by vibration and stirring during extraction of the drilling apparatus, which can lead to mixing and lack of preferred orientation of mineral grains in the deposits studied. As a result of friction of the deposits against the core barrel walls, a horizontally oriented depositional magnetic fabric may become inclined, with k_{min} deviating from the vertical. The deposits near the walls becoming inclined in the direction of the bottom of the hole. In extreme cases, as a result of suction of sediments into the core, we may have a situation where the k_{max} axis is oriented vertically, i.e. along the z-axis of the borehole core. Thus, the AMS method can help determine zones of deformed strata in borehole cores, which can increase the utility of any palaeomagnetic dating obtained.

Already earlier studies, e.g. Rosenbaum et al. (2000), had shown that AMS studies may be used to determine the degree of deformation in borehole cores, that can affect the proper interpretation of palaeomagnetic data. The research was carried out on the OL-92 borehole core drilled in Owens Lake in California. The core contains several zones of deformed lake deposits. Based on palaeomagnetic studies, several excursions of the magnetic field vector were interpreted. AMS samples were taken from levels representing field excursions named Pringle Falls, Jamaica/Biwa I, Blake and Mono Lake. For undisturbed core material, the average inclination value of the k_{min} axis is 84° and a standard deviation is 6.5° (Fig. 12). The inclination values of this axis do not fall below 80° . Disturbed deposits at depths of 19.0–12.5 m are characterized by an average inclination of the k_{min} axis of 66.5° and much greater standard deviation of 26.5° . Often, the inclination of this axis falls 80° . Similar relationships were observed at depths of 85.2–78.1 m. Both deformation zones coincide with the interpreted Mono Lake and Biwa excursions. The change in inclination of the k_{min} axis indicates a change in orientation of mineral grains in the deposits studied. Therefore, changes in the recorded inclination of the magnetic field vector cannot be interpreted as its short-term excursions over time.

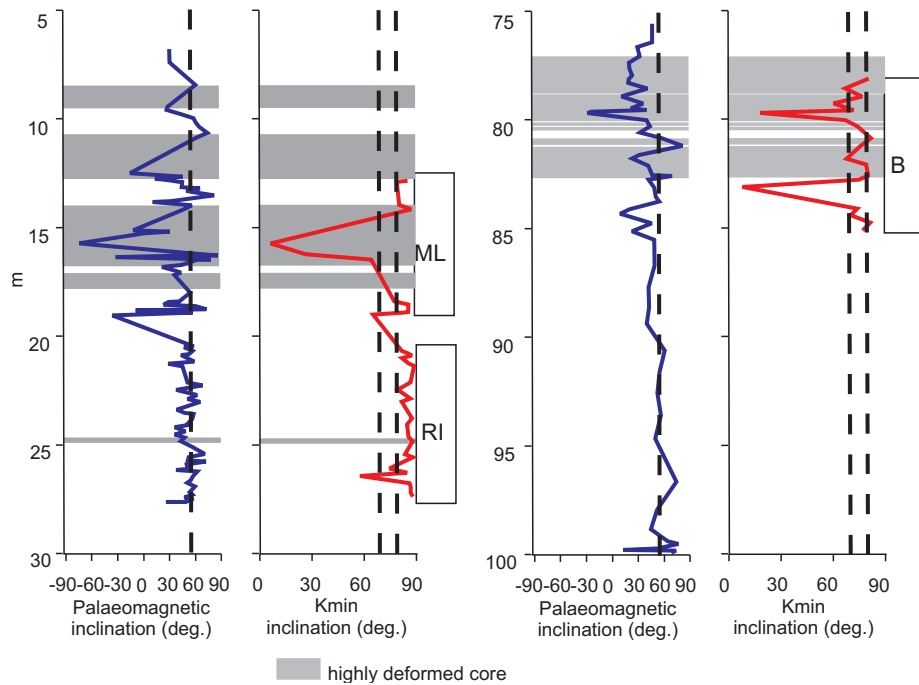


Fig. 12. Values of the inclination of the palaeomagnetic field vector (blue line) and the inclination of the kmin axis (red line) for selected sections of the OL-92 borehole core according to Rosenbaum et al. (2000); rectangles indicate the range of magnetic field excursions determined (ML – Mono Lake, B – Blake) and a borehole core segment with undeformed deposits (RI)

SUMMARY

The method of anisotropy of magnetic susceptibility has been widely used in studies of Quaternary deposits. It allows determination of the arrangement of mineral grains in the materials studied. AMS measurements are easy, low-cost and quick to perform. Compared to traditional methods such as determining the orientation of mineral grains in thin sections or measuring the longest axis of pebbles in glacial tills, they are characterized by a low error resulting from human factors. In Quaternary studies, AMS studies have been used to reconstruct the directions of transport of rock material, such as in loess or ice-

dammed deposits. Based on the arrangement of the principal axes of magnetic susceptibility, it is possible to determine the directions of ice-sheet movement and mechanisms of deposition of glacial tills and to reconstruct tectonic stress fields. This method is also useful for constraining data obtained from palaeomagnetic studies or for profiling sedimentary successions. The examples presented here show that this method can produce much new information for Quaternary sedimentary studies.

Acknowledgements. The author would like to thank the reviewers, D.J. Anastasio and P. Pruner, for all their comments and suggestions that improved this manuscript.

REFERENCES

- Almqvist, B.S.G., Bosshard, S.A., Hirt, A.M., Mattsson, H.B., Hetényi, G., 2012. Internal flow structures in columnar jointed basalt from Hrepphólar, Iceland: II. Magnetic anisotropy and rock magnetic properties. *Bulletin of Volcanology*, **74**: 1667–1681. <https://doi.org/10.1007/s00445-012-0622-0>
- Anastasio, D.J., Pazzaglia, F.J., Parés, J.M., Kodama, K.P., Berti, C., Fisher, J.A., Montanari, A., Carnes, L.K., 2021. Application of anisotropy of magnetic susceptibility (AMS) fabrics to determine the kinematics of active tectonics: examples from the Betic Cordillera, Spain, and the Northern Apennines, Italy. *Solid Earth*, **12**: 1125–1142. <https://doi.org/10.5194/se-12-1125-2021>
- Ankerstjerne, S., Iverson, N.R., Lagroix, F., 2015. Origin of a washboard moraine of the Des Moines Lobe inferred from sediment properties. *Geomorphology*, **248**: 452–463. <https://doi.org/10.1016/j.geomorph.2015.07.019>
- Baas, J.H., Hailwood, E.A., McCaffrey, W.D., Kay, M., Jones, R., 2007. Directional petrological characterisation of deep-marine sandstones using grain fabric and permeability anisotropy: methodologies, theory, application and suggestions for integration. *Earth-Science Reviews*, **82**: 101–142. <https://doi.org/10.1016/j.earscirev.2007.02.003>
- Balsamo, F., Storti, F., Piovano, B., Salvini, F., Cifelli, F., Lima, C., 2008. Time dependent structural architecture of subsidiary fracturing and stress pattern in the tip region of an extensional growth fault system, Tarquinia basin, Italy. *Tectonophysics*, **454**:

- turing and stress pattern in the tip region of an extensional growth fault system, Tarquinia basin, Italy. *Tectonophysics*, **454**: 54–69. <https://doi.org/10.1016/j.tecto.2008.04.011>
- Biedermann, A.R., 2018.** Magnetic Anisotropy in Single Crystals: a Review. *Geosciences*, **8**: 302. <https://doi.org/10.3390/geosciences8080302>
- Biedermann, A.R., Kunze, K., Hirt, A.M., 2018.** Interpreting magnetic fabrics in amphibole-bearing rocks. *Tectonophysics*, **722**: 566–576. <https://doi.org/10.1016/j.tecto.2017.11.033>
- Borradaile, G.J., Hamilton, T., 2004.** Magnetic fabrics may proxy as neotectonic stress trajectories, Polis rift, Cyprus. *Tectonics*, **23**: TC1001. <https://doi.org/10.1029/2002TC001434>
- Borradaile, G.J., Henry, B., 1997.** Tectonic applications of magnetic susceptibility and its anisotropy. *Earth-Science Reviews*, **42**: 49–93. [https://doi.org/10.1016/S0012-8252\(96\)00044-X](https://doi.org/10.1016/S0012-8252(96)00044-X)
- Borradaile, G.J., Jackson, M., 2010.** Structural geology, petrofabrics and magnetic fabrics (AMS, AARM, AIRM). *Journal of Structural Geology*, **32**: 1519–1551. <https://doi.org/10.1016/j.jsg.2009.09.006>
- Bradák-Hayashi, B., Biró, T., Horváth, E., Végh, T., Csillag, G., 2016.** New aspects of the interpretation of the loess magnetic fabric, Cérna Valley succession, Hungary. *Quaternary Research*, **86**: 348–358. <https://doi.org/10.1016/j.yqres.2016.07.007>
- Bradák, B., Seto, Y., Hyodo, M., Szeberényi, J., 2018a.** Relevance of ultrafine grains in the magnetic fabric of paleosols. *Geoderma*, **330**: 125–135. <https://doi.org/10.1016/j.geoderma.2018.05.036>
- Bradák, B., Ujvari, G., Seto, Y., Hyodo, M., Végh, T., 2018b.** A conceptual magnetic fabric development model for the Paks loess in Hungary. *Aeolian Research*, **30**: 20–31. <https://doi.org/10.1016/j.aeolia.2017.11.002>
- Bradák, B., Seto, Y., Chadima, M., Kovács, J., Tanos, P., Újvári, G., Hyodo, M., 2020.** Magnetic fabric of loess and its significance in Pleistocene environment reconstructions. *Earth-Science Reviews*, **210**: 103385. <https://doi.org/10.1016/j.earscirev.2020.103385>
- Butler, R.F., 1992.** Paleomagnetism: Magnetic Domains to Geologic Terranes. Blackwell Scientific Publications, Boston.
- Caricchi, C., Cifelli, F., Kissel, C., Sagnotti, L., Mattei, M., 2016.** Distinct magnetic fabric in weakly deformed sediments from extensional basins and fold-and-thrust structures in the Northern Apennine orogenic belt (Italy). *Tectonics*, **35**: 238–256. <https://doi.org/10.1002/2015TC003940>
- Chadima, M., Hansen, A., Hirt, A.M., Hrouda, F., Siemes, H., 2004.** Phyllosilicate preferred orientation as a control of magnetic fabric: evidence from neutron texture goniometry and low and high-field magnetic anisotropy (SE Rhenohercynian Zone of Bohemian Massif). *Special Publications, Geological Society*, **238**: 361–380. <https://doi.org/10.1144/GSL.SP.2004.238.01.1>
- Chlebowski, R., Gozik, P., Lindner, L., 2000.** Preliminary comparative characteristic of upper younger loesses in the Małopolska Upland (Poland) and the central basin of the Dnieper (Ukraine) on the basis of mineralogical studies (in Polish with English summary). *Biuletyn Państwowego Instytutu Geologicznego*, **393**: 1–19.
- Cifelli, F., Rossetti, F., Mattei, M., Hirt, A.M., Funicello, R., Torrici, F., 2004.** An AMS, structural and paleomagnetic study of quaternary deformation in eastern Sicily. *Journal of Structural Geology*, **26**: 29–46. [https://doi.org/10.1016/S0191-8141\(03\)00092-0](https://doi.org/10.1016/S0191-8141(03)00092-0)
- Cifelli, F., Mattei, M., Chadima, M., Hirt, A.M., Hansen, A., 2005.** The origin of tectonic lineation in extensional basins: combined neutron texture and magnetic analyses on undeformed clays. *Earth and Planetary Science Letters*, **235**: 62–78. <https://doi.org/10.1016/j.tecto.2008.08.008>
- Cifelli, F., Mattei, M., Chadima, M., Lenser, S., Hirt, A.M., 2009.** The magnetic fabric in “undeformed clays”: AMS and neutron texture analyses from the Rif Chain (Morocco). *Tectonophysics*, **466**: 79–88. <https://doi.org/10.1016/j.tecto.2008.08.008>
- Clark, G.K.C., 2005.** Subglacial processes. *Annual Review of Earth and Planetary Sciences*, **33**: 247–276. <https://doi.org/10.1146/annurev.earth.33.092203.122621>
- Collinson, D.W., 1983.** *Methods in Rock Magnetism and Palaeomagnetism*. Springer, Dordrecht. <https://doi.org/10.1007/978-94-015-3979-1>
- Černý, J., Melichar, R., Všianský, D., Drahekoupil, J., 2020.** Magnetic anisotropy of rocks: A new classification of inverse magnetic fabrics to help geological interpretations. *Journal of Geophysical Research: Solid Earth*, **125**: e2020JB020426. <https://doi.org/10.1029/2020JB020426>
- Dunlop, D.J., Özdemir, Ö., 1997.** *Rock Magnetism. Fundamentals and Frontiers*. Cambridge University Press. <https://doi.org/10.1017/cbo9780511612794>
- Dzierżek, J., Lindner, L., Kleindienst, U., Szymanek, M., Teodorski, A., 2022.** Wyspa lessowa Korzecka koło Chęciny; charakterystyka i warunki akumulacji lessu (in Polish). In: XXI Tere-nowe Seminarium Korelacja lessów i osadów glacialnych Polski i Ukrainy. Złodowacenia i interglacjały w Polsce – stan obecny i perspektywy badań, Chęciny 16–18 czerwca 2023 r. (eds. M. Łanczont, B. Holub and P. Mroczek): 29–31. *Interdyscyplinarne Seminarium Naukowe Glacjał i peryglacjał Europy środkowej pod tytułem: Metodyka rekonstrukcji zmian klimatu i środowiska zapisanych w pokrywach lessowych*. Jarosław, 6–8.10.22. Instytut Nauk o Ziemi i Środowisku Uniwersytetu Marii Curie-Skłodowskiej.
- Evans, M.E., Heller, F., 2003.** *Environmental Magnetism: Principles and Applications of Enviromagnetics*. Academic Press.
- Fleming, E.J., Lovell, H., Stevenson, C.T.E., Petronis, M.S., Benn, D.I., Hambrey, M.J., Fairchild, I.J., 2013a.** Magnetic fabrics in the basal ice of a surge type glacier. *Journal of Geophysical Research: Earth Surface*, **118**: 2263–2278. <https://doi.org/10.1002/jgrf.20144>
- Fleming, E.J., Stevenson, C.T.E., Petronis, M.S., 2013b.** New insights into the deformation of a Middle Pleistocene glacio-tectonised sequence in Norfolk, England through magnetic and structural analysis. *Proceedings of the Geologists' Association*, **124**: 834–854. <https://doi.org/10.1016/j.pgeola.2012.11.004>
- Fuller, M.D., 1962.** A magnetic fabric in till. *Geological Magazine*, **99**: 233–237. <https://doi.org/10.1017/S0016756800058271>
- Ge, J., Guo, Z., Zhao, D., Zhang, Y., Wang, T., Yi, L., Deng, C., 2014.** Spatial variations in paleowind direction during the last glacial period in north China reconstructed from variations in the anisotropy of magnetic susceptibility of loess deposits. *Tectonophysics*, **629**: 353–361. <https://doi.org/10.1016/j.tecto.2014.07.002>
- Gentoso, M.J., Evenson, E.B., Kodama, K.P., Iverson, N.R., Alley, R.B., Berti, C., Kozłowski, A., 2012.** Exploring till bed kinematics using AMS magnetic fabrics and pebble fabrics: the Weedsport drumlin field, New York State, USA. *Boreas*, **41**: 31–41. <https://doi.org/10.1111/j.1502-3885.2011.00221.x>
- Hooyer, T.S., Iverson, N.R., Lagroix, F., Thomason, F., 2008.** Magnetic fabric of sheared till: a strain indicator for evaluating the bed deformation model of glacier flow. *Journal of Geophysical Research*, **113**: F02002. <https://doi.org/10.1029/2007JF000757>
- Hopkins, N.R., Evenson, E.B., Kodama, K.P., Kozłowski, A., 2015.** An anisotropy of magnetic susceptibility (AMS) investigation of the till fabric of drumlins: support for an accretionary origin. *Boreas*, **45**: 100–108. <https://doi.org/10.1111/bor.12138>
- Hopkins, N.R., Kleman, J., Evenson, E.B., Kodama, K.P., 2016.** An anisotropy of magnetic susceptibility (AMS) fabric record of till kinematics within a Late Weichselian low Baltic till, southern Sweden. *Boreas*, **45**: 846–860. <https://doi.org/10.1111/bor.12192>
- Hrouda, F., 1982.** Magnetic anisotropy of rocks and its application in geology and geophysics. *Geophysical Surveys*, **5**: 37–82. <https://doi.org/10.1007/BF01450244>
- Hrouda, F., 2007.** Magnetic susceptibility, anisotropy. In: *Encyclopedia of Geomagnetism and Paleomagnetism* (eds. D. Gubbins and E. Herrero-Bervera): 546–560. Springer, Dordrecht. <https://doi.org/10.1007/978-1-4020-4423-6>

- Hrouda, F., Ježek, J., 2016. Role of single-domain magnetic particles in creation of inverse magnetic fabrics in volcanic rocks: qa mathematical model study. *Studia Geophysica et Geodaetica*, **61**: 145–161. <https://doi.org/10.1007/s11200-015-0675-6>
- Hrouda, F., Chadima, M., Ježek, J., Kadlec, J., 2018. Anisotropies of in-phase, out-of phase, and frequency-dependent susceptibilities in three loess/palaeosol profiles in the Czech Republic; methodological implications. *Studia Geophysica et Geodaetica*, **62**: 272–290. <https://doi.org/10.1007/s11200-017-0701-y>
- Hus, J.J., 2003. The magnetic fabric of some loess/paleosol deposits. *Physics and Chemistry of the Earth*, **28**: 689–699. [https://doi.org/10.1016/S1474-7065\(03\)00128-1](https://doi.org/10.1016/S1474-7065(03)00128-1)
- Ising, G., 1942. *Arkiv för matematik. Astronomi och Fysik*, **29A**(5).
- Ives, L.R.W., 2016. Magnetic mineralogy and fabrics of small-scale glacial flutes, Múlajökull and Breixamerkurjökull, Iceland. Graduate Theses and Dissertations, 14977. <http://lib.dr.iastate.edu/etd/14977>
- Jelinek, V., 1977. The statistical theory of measuring anisotropy of magnetic susceptibility of rocks and its application. *Geofyzika*, s.p. Brno.
- Jelinek, V., 1981. Characterization of the magnetic fabric of rocks. *Tectonophysics*, **79**: 63–67. [https://doi.org/10.1016/0040-1951\(81\)90110-4](https://doi.org/10.1016/0040-1951(81)90110-4)
- Jordanova, N., Jordanova, D., Karloukovski, V., 1996. Magnetic fabric of Bulgarian loess sediments derived by using various sampling techniques. *Studia Geophysica et Geodaetica*, **40**: 36–49. <https://doi.org/10.1007/BF02295904>
- King, R.F., 1955. The remanent magnetism of artificially deposited sediments. *Geophysical Journal International*, **7** (s3): 115–134. <https://doi.org/10.1111/j.1365-246X.1955.tb06558.x>
- Kissel, C., Laj, C., Lehman, B., Labyrie, L., Bout-Roumaizilles, V., 1997. Changes in the strength of the Iceland–Scotland Overflow Water in the last 200,000 years: evidence from magnetic anisotropy analysis of core SU90-33. *Earth and Planetary Science Letters*, **152**: 25–36. [https://doi.org/10.1016/S0012-821X\(97\)00146-5](https://doi.org/10.1016/S0012-821X(97)00146-5)
- Król, E., Wacheccka-Kotkowska, L., 2015. Anisotropy of magnetic susceptibility as a potential tool of palaeocurrent direction of the glacial sediments in the Piotrków Trybunalski, Radomsko and Przedbórz area (Central Poland). *Acta Geographica Lodziana*, **103**: 79–98.
- Kuehn, R., Hirt, A.M., Biedermann, A.R., Leiss, B., 2019. Quantitative comparison of microfabric and magnetic fabric in black shales from the Appalachian plateau (western Pennsylvania, U.S.A.). *Tectonophysics*, **765**: 161–171. <https://doi.org/10.1016/j.tecto.2019.04.013>
- Lagroix, F., Banerjee, S.K., 2004. Cryptic post-depositional reworking in aeolian sediments revealed by the anisotropy of magnetic susceptibility. *Earth and Planetary Science Letters*, **224**: 453–459. <https://doi.org/10.1016/j.epsl.2004.05.029>
- Lam, K.P., Hitchcock, A.P., Obst, M., Lawrence, J.R., Swerhone, G.D.W., Leppard, G.G., Tyliszczak, T., Karunakaran, C., Wang, J., Kaznatcheev, K., Bazyliniski, D.A., Lins, U., 2010. Characterizing magnetism of individual magnetosomes by X-ray magnetic circular dichroism in a scanning transmission X-ray microscope. *Chemical Geology*, **270**: 110–116. <https://doi.org/10.1016/j.chemgeo.2009.11.009>
- Li, J., Pan, Y., Liu, O., Yu-Zhang, K., Menguy, N., Che, R., Qin, H., Lin, W., Wu, W., Petersen, N., Yang, X., 2010. Biomineralization, crystallography and magnetic properties of bullet-shaped magnetite magnetosomes in giant rod magnetotactic bacteria. *Earth and Planetary Science Letters*, **293**: 368–376. <https://doi.org/10.1016/j.epsl.2010.03.007>
- Liu, Q., Roberts, A.P., Larrasoana, J.C., Banerjee, S.K., Guyodo, Y., Tauxe, L., Oldfield, L., 2012. Environmental magnetism: principles and applications. *Reviews of Geophysics*, **0**, RG4002. <https://doi.org/10.1029/2012RG000393>
- Liu, W.M., Sun, J.M., 2012. High-resolution anisotropy of magnetic susceptibility record in the central Chinese Loess Plateau and its paleoenvironment implications. *Science China. Earth Sciences*, **55**: 488–494. <https://doi.org/10.1007/s11430-011-4354-3>
- Liu, X., Xu, T., Liu, T., 1988. The Chinese loess in Xifeng, II. A study of anisotropy of magnetic susceptibility of loess from Xifeng. *Geophysical Journal International*, **92**: 349–353. <https://doi.org/10.1111/j.1365-246X.1988.tb01147.x>
- Liu, B., Saito, Y., Yamazaki, T., Abdeldayem, A., Oda, H., Hori, K., Zhao, Q., 2001. Paleocurrent analysis for the Late Pleistocene–Holocene incised-valley fill of the Yangtze delta, China by using anisotropy of magnetic susceptibility data. *Marine Geology*, **176**: 175–189. [https://doi.org/10.1016/S0025-3227\(01\)00151-7](https://doi.org/10.1016/S0025-3227(01)00151-7)
- Lüneburg, C.M., Lampert, S.A., Lebit, H.D., Hirt, A.M., Casey, M., Lowrie, W., 1999. Magnetic anisotropy, rock fabrics and finite strain in deformed sediments of SW Sardinia (Italy). *Tectonophysics*, **307**: 51–74. [https://doi.org/10.1016/S0040-1951\(99\)00118-3](https://doi.org/10.1016/S0040-1951(99)00118-3)
- Maffione, M., Pucci, S., Sagnotti, L., Speranza, F., 2012. Magnetic fabric of Pleistocene continental clays from the hanging-wall of an active low-angle normal fault (Altotiberina Fault, Italy). *International Journal of Earth Sciences*, **101**: 849–861. <https://doi.org/10.1007/s00531-011-0704-9>
- Marks, L., Dzierżek, J., Janiszewski, R., Kaczorowski, J., Lindner, L., Majecka, A., Makos, M., Szymanek, M., Tołoczko-Pasek, A., Woronko, B., 2016. Quaternary stratigraphy and palaeogeography of Poland. *Acta Geologica Polonica*, **66**: 403–427. <https://doi.org/10.1515/aggp-2016-0018>
- Mattei, M., Sagnotti, L., Faccenna, C., Funicello, R., 1997. Magnetic fabric of weakly deformed clay-rich sediments in the Italian peninsula: relationship with compressional and extensional tectonics. *Tectonophysics*, **271**: 107–122. [https://doi.org/10.1016/S0040-1951\(96\)00244-2](https://doi.org/10.1016/S0040-1951(96)00244-2)
- McCracken, R.G., Iverson, N.R., Benediktsson, Í.Ö., Schomacker, A., Zoet, L.K., Johnson, M.D., Hooyer, T.S., Ingólfsson, Ó., 2016. Origin of the active drumlin field at Múlajökull, Iceland: New insights from till shear and consolidation patterns. *Quaternary Science Reviews*, **148**: 243–260. <https://doi.org/10.1016/j.quascirev.2016.07.008>
- Narloch, W., Werner, W., Tylmann, K., 2021. Deformation mechanisms and kinematics of a soft sedimentary bed beneath the Scandinavian Ice Sheet, north-central Poland, revealed by magnetic fabrics. *Sedimentary Geology*, **416**: 105862. <https://doi.org/10.1016/j.sedgeo.2021.105862>
- Nawrocki, J., Polechońska, O., Boguckij, A., Łanczont, M., 2006. Palaeowind directions recorded in the youngest loess in Poland and western Ukraine as derived from anisotropy of magnetic susceptibility measurements. *Boreas*, **35**: 266–271. <https://doi.org/10.1111/j.1502-3885.2006.tb01156.x>
- Nawrocki, J., Bogucki, A.B., Gozhik, P., Łanczont, M., Pańczyk, M., Standzikowski, K., Komar, M., Rosowiecka, O., Tomeniuk, O., 2019. Fluctuations of the Fennoscandian Ice Sheet recorded in the anisotropy of magnetic susceptibility of periglacial loess from Ukraine. *Boreas*, **48**: 940–952. <https://doi.org/10.1111/bor.12400>
- Nowaczyk, B., 2002. Lithological and geomorphological record of aeolian activity in Poland in the last 30 000 years. *Czasopismo Geograficzne*, **73**: 275–311.
- Obersteinová, T., 2016. Magnetic Fabric of Selected Loess-paleosol Sequences in Southern Moravia and Central Bohemia (in Czech with English summary). Ph.D. Thesis, Charles University.

- Oliva-Urcia, B., Román-Berdiel, T., Casas, A.M., Pueyo, E.L., Osácar, C., 2010.** Tertiary compressional overprint on Aptian-Albian extensional magnetic fabrics, North Pyrenean Zone. *Journal of Structural Geology*, **32**: 362–376. <https://doi.org/10.1016/j.jsg.2010.01.009>
- Parés, J.M., 2015.** Sixty years of anisotropy of magnetic susceptibility in deformed sedimentary rock. *Frontiers in Earth Science*, **3**: 1–12. <https://doi.org/10.3389/feart.2015.00004>
- Parés, J.M., van der Pluijm, B.A., 2002.** Evaluating magnetic lineations (AMS) in deformed rocks. *Tectonophysics*, **350**: 283–298. [https://doi.org/10.1016/S0040-1951\(02\)00119-1](https://doi.org/10.1016/S0040-1951(02)00119-1)
- Parés, J.M., van der Pluijm, B.A., 2003.** Magnetic fabrics and strain in pencil structures of the Knobs Formation, valley and ridge province, US Appalachians. *Journal of Structural Geology*, **25**: 1349–1358. [https://doi.org/10.1016/S0191-8141\(02\)00197-9](https://doi.org/10.1016/S0191-8141(02)00197-9)
- Porreca, M., Mattei, M., 2012.** AMS fabric and tectonic evolution of Quaternary intramontane extensional basins in the Picentini Mountains (southern Apennines, Italy). *International Journal of Earth Sciences*, **101**: 863–877. <https://doi.org/10.1007/s00531-011-0670-2>
- Rees, A.I., 1961.** The effect of water currents on the magnetic remanence and anisotropy of susceptibility of some sediments. *Geophysical Journal of the Royal Astronomical Society*, **5**: 235–251. <https://doi.org/10.1111/j.1365-246X.1961.tb00431.x>
- Rees, A.I., 1964.** Measurements of natural remanent magnetism and anisotropy of susceptibility of some Swedish glacial silt. *Geophysical Journal of the Royal Astronomical Society*, **8**: 356–369. <https://doi.org/10.1111/j.1365-246X.1964.tb03857.x>
- Rees, A.I., 1965.** The use of anisotropy of magnetic susceptibility in the estimation of sedimentary fabric. *Sedimentology*, **4**: 257–271. <https://doi.org/10.1111/j.1365-3091.1965.tb01550.x>
- Rees, A.I., 1966.** The effect of depositional slopes on the anisotropy of magnetic susceptibility of laboratory deposited sands. *The Journal of Geology*, **74**: 856–867. <https://doi.org/10.1086/627216>
- Rochette, P., Jackson, M., Aubourg, C., 1992.** Rock magnetism and the interpretation of anisotropy of magnetic susceptibility. *Reviews of Geophysics*, **30**: 209–226. <https://doi.org/10.1029/92RG00733>
- Rosenbaum, J., Reynolds, R., Smoot, J., Meyer, R., 2000.** Anisotropy of magnetic susceptibility as a tool for recognizing core deformation: reevaluation of the paleomagnetic record of Pleistocene sediments from drill hole OL-92, Owens Lake, California. *Earth and Planetary Science Letters*, **178**: 415–424. [https://doi.org/10.1016/S0012-821X\(00\)00077-7](https://doi.org/10.1016/S0012-821X(00)00077-7)
- Schmidt, V., Hirt, A.M., Leiss, B., Burlini, L., Walter, J.M., 2009.** Quantitative correlation of texture and magnetic anisotropy of compacted calcite–muscovite aggregates. *Journal of Structural Geology*, **31**: 1062–1073. <https://doi.org/10.1016/j.jsg.2008.11.012>
- Schöbel, S., de Wall, H., Rolf, C., 2013.** AMS in basalts: is there a need for prior demagnetization? *Geophysical Journal International*, **195**: 1509–1518. <https://doi.org/10.1093/gji/ggt325>
- Shumway, J.R., Iverson, N.R., 2009.** Magnetic fabrics of the Douglas Till of the Superior lobe: exploring bed deformation kinematics. *Quaternary Science Reviews*, **28**: 107–119. <https://doi.org/10.1016/j.jsg.2008.11.012>
- Tang, Z., Huang, B., Dong, X., Ji, J., Ding, Z., 2012.** Anisotropy of magnetic susceptibility of the Jingou River section: implications for late Cenozoic uplift of the Tian Shan. *Geochemistry, Geophysics, Geosystems*, **13**: Q03022. <https://doi.org/10.1029/2011GC003966>
- Tarling, D.H., Hrouda, F., 1993.** *The Magnetic Anisotropy of Rocks*. 218 Chapman and Hall, London, Glasgow, New York, Tokyo, Melbourne, Madras.
- Tauxe, L., 2005.** *Lectures in Paleomagnetism*. Electronic version. <http://earthref.org/MAGIC/books/Tauxe/2005/>
- Taylor, S.N., Lagroix, F., 2015.** Magnetic anisotropy reveals the depositional and post-depositional history of a loess-paleosol sequence at Nussloch (Germany): AMS of Nussloch loess-paleosol sequence. *Journal of Geophysical Research: Solid Earth*, **120**: 2859–2876. <https://doi.org/10.1002/2014JB011803>
- Teodorski, A., Dzierżek, J., Ziółkowski, P., 2021.** Reconstruction of subglacial depositional conditions based on the anisotropy of magnetic susceptibility: an example from Dębe (Central Poland). *Journal of Quaternary Science*, **36**: 391–402. <https://doi.org/10.1002/jqs.3284>
- Thomason, J.F., Iverson, N.R., 2009.** Deformation of the Batestown till of the Lake Michigan lobe, Laurentide ice sheet. *Journal of Glaciology*, **55**: 131–146. <https://doi.org/10.3189/002214309788608877>
- Wang, R., Løvlie, R., 2010.** Subaerial and subaqueous deposition of loess: experimental assessment of detrital remanent magnetization in Chinese loess. *Earth and Planetary Science Letters*, **298**: 394–404. <https://doi.org/10.1016/j.epsl.2010.08.019>
- Xie, X., Xian, F., Wu, Z., Kong, X., Chang, Q., 2016.** Asian Monsoon variation over the late Neogene–early Quaternary recorded by Anisotropy of Magnetic Susceptibility (AMS) from Chinese loess. *Quaternary International*, **399**: 183–189. <https://doi.org/10.1016/j.quaint.2015.04.061>
- Yang, T., Zhao, X., Petronotis, K., Dekkers, M. J., Xu, H., 2019.** Anisotropy of magnetic susceptibility (AMS) of sediments from holes U1480E and U1480H, IODP Expedition 362: Sedimentary or Artificial Origin and Implications for Paleomagnetic Studies. *Geochemistry, Geophysics, Geosystems*, **20**: 5192–5215. <https://doi.org/10.1029/2019GC008721>
- Zeeden, C., Hambach, U., Händel, M., 2015.** Loess magnetic fabric of the Krems-Wachtberg archaeological site. *Quaternary International*, **372**: 188–194. <https://doi.org/10.1016/j.quaint.2014.11.001>
- Zhang, R., Kravchinsky, V.A., Zhu, R., Yue, L., 2010.** Paleomonsoon route reconstruction along a W–E transect in the Chinese Loess Plateau using the anisotropy of magnetic susceptibility: summer monsoon model. *Earth and Planetary Science Letters*, **299**: 436–446. <https://doi.org/10.1016/j.epsl.2010.09.026>